Chapter 11
Development of Skeletal Drug Delivery System Based on Apatite/Collagen Composite Cement

Makoto Otsuka

Abstract Since bone resorption and formation occur repeatedly within the functional units referred to as bone multicellular units, uncoupling between bone resorption by osteoclasts and bone formation by osteoblasts causes an absolute decrease in the amount of bone in osteoporosis. For that reason, it is necessary to fully understand the remodeling characteristics of bone grafts by osteoclasts and osteoblasts to high-bioactive materials. We have, therefore, prepared hydroxyapatite (HAp) and collagen composites to improve bioaffinity through the interaction between materials and bone cells for applications in drug delivery devices. Apatite/collagen composite cements could be applied to artificial bone drug delivery systems without drug inactivation caused by high pressure and those that exhibit long-term slow drug release in vitro and high in vivo biocompatibility in osteoporosis model rats. On the other hand, geometrical structure of pores in implantable artificial bone has been proven successful in bone generation, since bone-related cells can be cultured more readily in interconnected porous materials, such as coral-modified implant made by calcium phosphate. Interconnective pores in coral-like material are therapeutically effective in bone regeneration within the body through the introduction of bone cells and capitally blood vessels as a scaffold for bone cells to spread and proliferate. The interconnective porous biomaterials are, therefore, developed based on self-setting apatite/collagen composite cement as materials with enhanced biocompatibility and drug delivery capability. Since the drug release rate from the composite device could be controlled by various geometrical factors, the relationship between drug-release rate and number of the macropores was investigated by in vitro dissolution test. Bioaffinity of the interconnective porous biomaterials of apatite/collagen composite cement was examined in rat models using X-ray computed tomography.

M. Otsuka (✉)
Faculty of Pharmacy, Research Institute of Pharmaceutical Science, Musashino University, 1-1-20 Shinmachi, 202-8585 Nishi-Tokyo, Tokyo, Japan
e-mail: motsuka@musashino-u.ac.jp

B. Ben-Nissan (ed.), *Advances in Calcium Phosphate Biomaterials*, Springer Series in Biomaterials Science and Engineering 2, DOI 10.1007/978-3-642-53980-0_11,

Keywords Apatite cement • Apatite/collagen composite • Biocompatibility • Drug delivery • Nanostructure • Cell scaffold

11.1 Introduction

In order to develop highly bioactive bone materials, it is vital that the characteristics of bone graft remodeling by osteoclasts and osteoblasts are fully understood. Since bone resorption and formation occur repeatedly in the functional units called bone multicellular units, which maintain the dynamic equilibrium of mineral density in normal bone [1], uncoupling between bone resorption by osteoclasts and bone formation by osteoblasts causes an absolute decrease in the amount of bone in osteoporosis. Bioactive ceramics with excellent bioaffinity, such as hydroxyapatite (HAp), β-tricalcium phosphate, and bioglass ceramics, are developed and can directly connect with bone [2]. However, the materials currently used as artificial bones possesses characteristics that are inadequate when compared to natural bone such as their brittle nature and poor mechanical strength. The material could also remain in the bone for an extended period because their chemical composition and geometrical structure are very different from natural bone and they exhibit lower bioaffinity [2].

On the other hand, a HAp/collagen composite with a nanostructure which is similar to natural bone was realized by Miyamoto et al. [3] and Kikuchi et al. [4, 5] and they reported that apatite and collagen were self-organizing and formed nanostructure composites by a simultaneous titration coprecipitation method and concluded that the molecular interaction between apatite and collagen induced formation of nanostructure particles, which has similar characteristics and biocompatibility to natural bone. John et al. [6] prepared apatite/collagen composite by using collagen sponge and investigated its suitability for bone repair applications. The results indicated that the bio-mimic materials had significantly high bioaffinity with natural bone after implantation and the molecular level structure of HAp/collagen composites is a very important factor for the biocompatibility of artificial bone in vivo. We have, therefore, developed self-setting HAp/collagen composite cement to improve bioaffinity by enhancing the interaction between the composites and bone cells for applications in drug delivery and cell scaffold devices [7].

11.2 Artificial Bone Cements Based on Self-Setting Apatite/Collagen Composite Cements (AC)

11.2.1 Physicochemical Prosperities of the AC

To develop an artificial self-setting bone cement with almost the same chemical formulation (80 % HAp and 20 % collagen) as natural bone, the AC was prepared

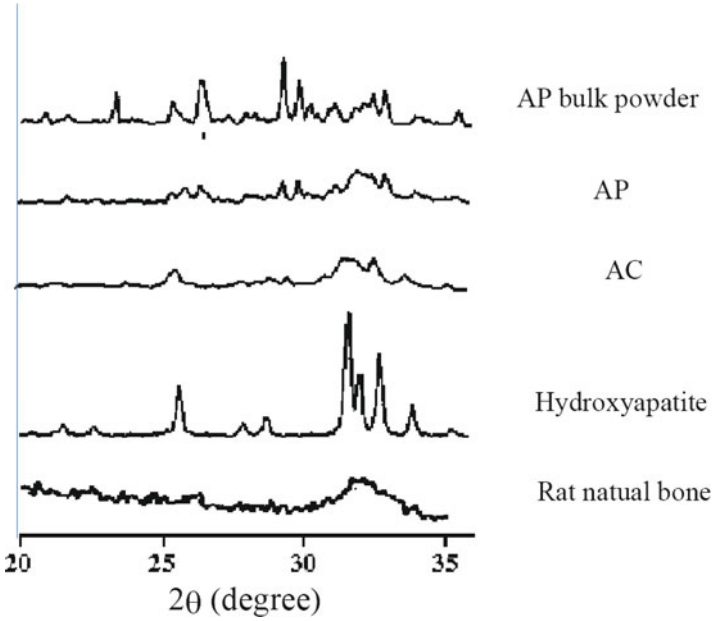

Fig. 11.1 X-ray diffraction profiles of self-setting apatite cement bulk powder (AP) and self-setting apatite/collagen composite cement (AC)

as follows: firstly, self-setting apatite cement bulk powder (AP) consisting of an equimolar mixture of tetracalcium phosphate (TECP, $Ca_4(PO_4)_2O$) and dicalcium phosphate dihydrate (DCPD, $CaHPO_4{\cdot}2H_2O$) was prepared by grinding in an agate vibration mixer mill [8–10]. The AC bulk powder was obtained by grinding the AP powder with 20 % type I bovine collagen in the vibration mixer mill. The AP or AC bulk powder (0.500 g) was mixed homogeneously with 0.20 mL of 11 mM phosphoric acid. The final paste was poured into a plastic mold and stored at 37 °C and 100 % relative humidity for 24 h.

The X-ray powder diffraction (XRD) profiles of the sample cements (Fig. 11.1) were measure to evaluate the test material characteristics as an index of bioaffinity. The fresh fixed AP cements showed typical diffraction peaks of HAp at $2\theta = 31.8$ and 32.8° with additional peaks at $2\theta = 28.9$ and 29.5° due to TECP and at $2\theta = 26.5°$ due to DCPD. The XRD results indicated that the majority of metastable calcium phosphates, DCPD and TECP, transformed into low-crystallinity HAp, but some parts of DCPD and TECP did not transform and remained in the cements. In contrast, the XRD profiles of AC had broad peaks at 31–33° due to bone-like HAp and no peaks due to TECP and DCPD (Fig. 11.1). The results also suggested that crystalline transformation of AP is accelerated by the addition of collagen and mechanical treatment. The transformed apatite structure in the AC was similar to natural bone apatite with low crystallinity reported by Kikuchi et al. [4], because the bone-like nano-apatite crystals precipitated out on collagen matrices during setting

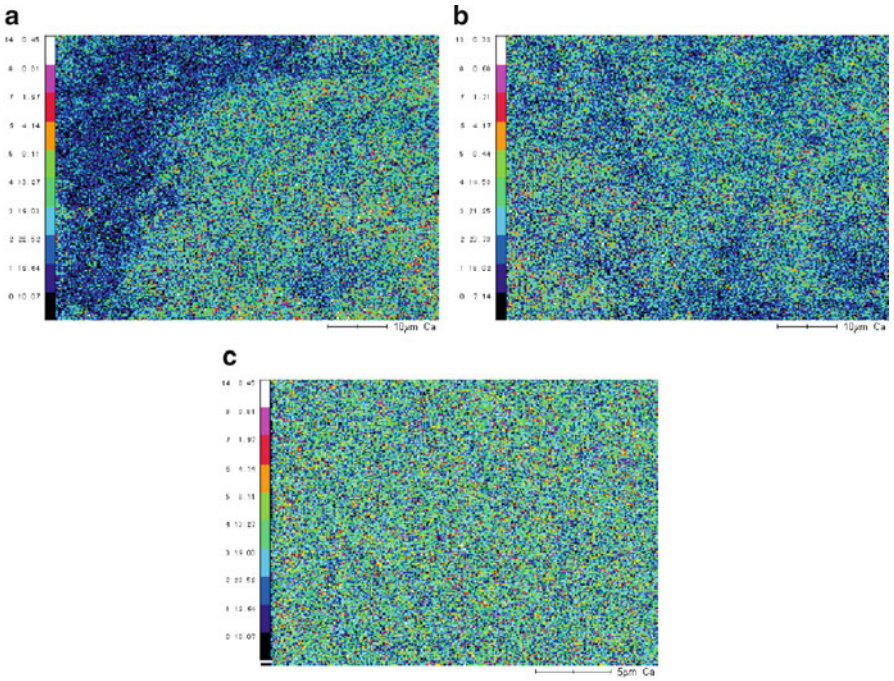

Fig. 11.2 Effects of grinding on element dispersibility of the AC by electron probe microanalyzer

time after mixing the solution. Chhettry et al. [8] reported the relationship between crystallinity and solubility of bone-like carbonated apatite and demonstrated that natural bone apatite had low crystallinity and high solubility. Therefore, the apatite in the AC might have high solubility and high biocompatibility.

Scanning electron microscopy (SEM) and electron probe microanalyzer (EPMA) were performed to characterize element dispensability in the AC [7]. The SEM of AC without grinding showed a rough surface and large particles (more than 20 μm particles in diameter), indicating that the cement was a heterogeneous system. In contrast, AC with grinding showed a smooth surface consisting of particles less than 1–2 μm in diameter.

The natural bone had a smooth surface with cracks. The result of mapping of calcium by EPMA suggested that there are calcium rich and less part in the AC without grinding (Fig. 11.2a). The calcium ion distribution in the AC (Fig. 11.2b) was more homogeneous than that in the AC without grinding, and the calcium ion homogeneity was almost the same as that of natural bone (Fig. 11.2c). These results indicated that AC without grinding had a heterogeneous structure in which collagen and calcium phosphates were not mixed uniformly. On the other hand, calcium and phosphates were dispersed homogeneously at the nanoscale in the cement as well as in the natural bone.

The result indicated that the raw materials of the apatite cement, such as DCPC and TECP, were micronized by mechanical energy during grinding in the vibration

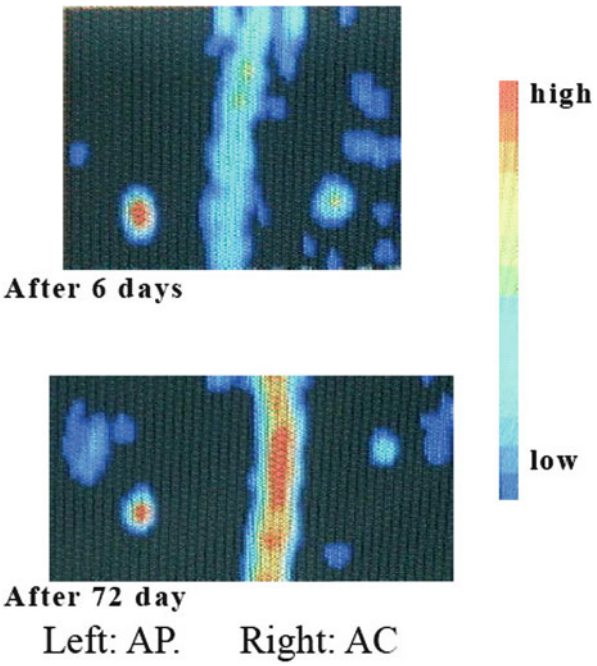

Fig. 11.3 Microradiogram of implanted AP and AC cements in rats by DEXA

mill and distributed into collagen matrices. Then, the micronized DCPD and TECP dissolved and recrystallized to nanoparticle apatite on collagen matrices. Since apatite formation of cement was catalyzed on collagen matrices, almost 100 % of calcium phosphate might be transformed to apatite.

11.2.2 Biodegradation of the AC in Rats

AC cements were implanted into the backs of rats and the density measured using bone mineral densitometry. Microradiograms of the AP and AC (Fig. 11.3) were measured by dual energy X-ray absorptiometry after implant in the rats, and the cement mineral content (BMC) was evaluated based on the microradiograms. The BMC of the implanted cements decreased with time, indicating that the cement was gradually bioabsorbed. Bioabsorption rates of the implanted cements (Fig. 11.4a) were dependent on the quality of cement (cement formulation). The BMCs of both of the AC and AP decrease over time, and the BMC of the AC was found to be significantly lower than that of the AP.

The effect of grinding on the BMC of the implanted cements (Fig. 11.4b) revealed the concentration of BMC decreases over time regardless of whether grinding was performed. The concentration of BMC in AC without grinding was always found to be lower than that of the AC.

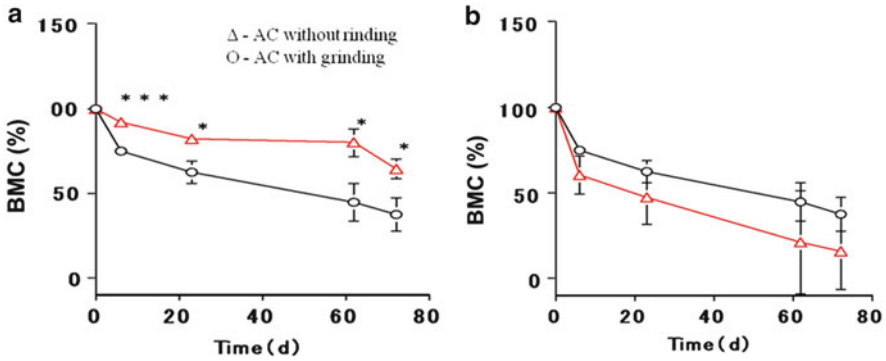

Fig. 11.4 Effects of cement formulation on the BMC of AP and AC cements by DEXA

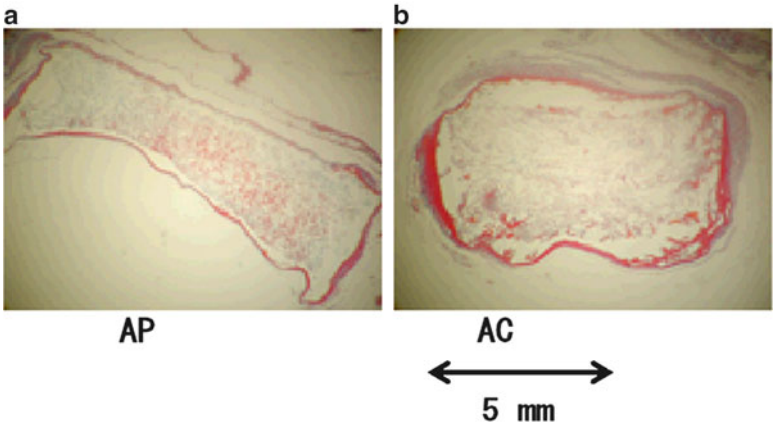

Fig. 11.5 Cross-section micrographs of (**a**) AP and (**b**) AC cements after 72 days of implantation

The results of the AP and AC suggested that the biodegradation rate was dependent on the cement quality and geometrical structure, and the rate can be shown as AP < AC < AC without grinding. The biodegradation rate of the AP was found to be the slowest as it is composed entirely of pure inorganic material. On the contrary, by having a nanoscale heterogeneous structure consisting of 80 % apatite and 20 % collagen, the AC without grinding had the highest biodegradation rate (Fig. 11.2a, d). The decreasing BMC behavior of the AC was found to be between those of the AP and the AC without grinding. This is mainly due to a decrease in the particle size of the cement and bone-like cells penetrating into the cement after implantation.

Figure 11.5 shows the micrographs of the cross section of the demineralized sample cement blocks after 72 days of implantation in soft tissue. The AP (Fig. 11.5a) kept its original diameter (6 mm) in soft tissues after implantation. A slight reduction in thickness was also observed as the organic components have penetrated into the cement. The data from the in vivo experiment showed shrinkage

in the diameter of AC by approximately 30 %, while an increase in thickness was recorded (Fig. 11.5b). In contrast, AC without grinding (data not shown) was totally absorbed and no traces of the cement were discovered in the soft tissues.

These results indicated that the BMC changes and their bioaffinity were significantly dependent on the quality of apatite and the nano-geometrical structure in the cement. The biodegradation rate of the AC could be controlled by the cement formulation and the geometrical structure.

11.3 Drug Delivery System Based on Apatite/Collagen Composite Cements

In order to develop bone regenerative artificial bone systems, it is necessary that bone growth factors are loaded in bioactive artificial bone matrices and slowly releases through time. Shiraki et al. [9] reported that metacarpal bone mineral density was increased in osteoporosis through the administration of menatetrenone, vitamin K_2 (VK2, anti-osteoporosis drug). They indicated that VK2 prevented trabecular bone loss and the occurrence of bone fractures [10] in osteoporosis. Therefore, the VK2 is selected as a model drug and loaded in the bone cement matrices to develop a drug delivery system.

11.3.1 Therapeutic Effect of Drug Delivery System of the AC on Bone Mass in the Rats

Apatite/collagen composite cements loaded with bone growth factors is believed to have a better biocompatibility than simple artificial bone implants. The effects of anti-osteoporosis drug on bone mass were investigated in the osteoporosis rats. The AC cement bulk powder was prepared by grinding 80 % AP with 20 % collagen for 20 min. After that, the bulk powder (0.500 g) of the AP or AC was mixed homogeneously with 0.20 mL of 11 mM phosphoric acid, then 10 mg of VK2 powders were mixed, and the final paste was poured into a plastic mold and stored at 37 °C and 100 % relative humidity for 24 h. Three types of the drug delivery devices were developed [7]:

1. APK – VK2 loaded in the AP
2. ACPK – VK2 loaded in the AC without grinding
3. ACGK – VK2 loaded in the AC with grinding

After the VK2-loaded devices were implanted in the osteoporosis rats, the BMC was measured as index of biodegradation rate. Figure 11.6 shows the effects of VK2 on BMC of apatite/collagen cements implanted in osteoporosis rats. The BMC profile of the ACGK was significantly higher than those of the ACPK and

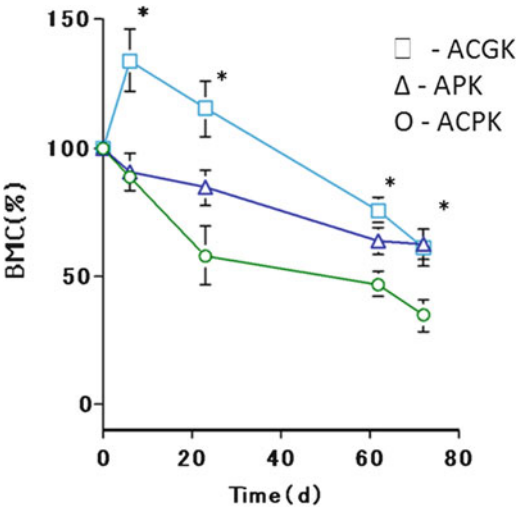

Fig. 11.6 Effects of cement formulation on BMC of AP and AC cements containing VK2

APK. On the other hand, the microstructure of ACGK was significantly different from APK, and that difference was drastically affected by the duration of the experimental. For ACGK, the amount of BMC reached its peak at day 7. ACPK and APK recorded the highest and slowest degradation rates of BMC, respectively. At day 21, the amount of BMC present can be shown as ACGK > APK > ACPK.

The micrographs of the cross sections of the apatite/collagen cements containing VK2 taken after 72 days of implantation were shown in Fig. 11.7. After implantation, it was discovered that the APK cement had undergone deformation but there are no evidence to suggest penetration of organic components into the cement material (Fig. 11.7a). Likewise for the ACPK cement with a reduction in diameter but an increase in thickness, the shape of the ACGK cement had been completely distorted after 72 days (Fig. 11.7b).

The BMC result of the cements loaded with VK2 suggests that their formulation has a significant effect on the rate of biodegradation. After 72 days, the ACGK cement recorded an increase in BMC, which was also higher than the ACPK cement (Fig. 11.6). The organic components had penetrated deeply into the center of the ACGK (Fig. 11.7b). These results suggested that the changes in BMC were more dynamic for the ACGK than the ACPK cement. As shown in the X-ray diffraction results, grinding the apatite/collagen composite cement can lead to a crystalline structure that is more or less the same as natural bone; this could have an influence on the release of bone growth factors such as VK2 and the regeneration and absorption of bone during the experimental period.

The BMC profile of AC suggests the quick release of VK2 may encourage organic components to penetrate the ACPK cement and stimulate the activity of the surrounding cells. Observations made from the ACPK micrographs revealed organic components had penetrated into the cement and causing the shape the cement to totally deform. On the other hand, a complete absorption of AC was observed.

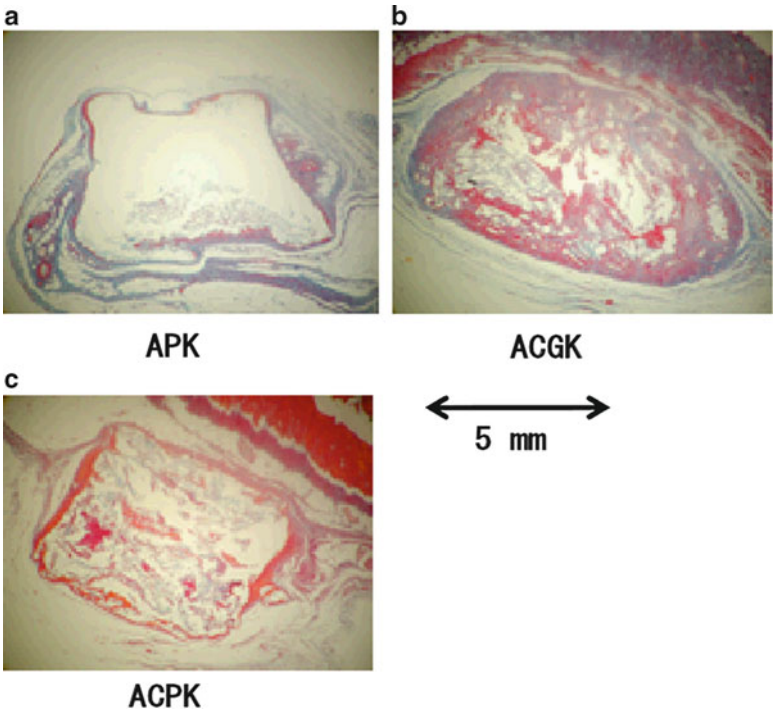

Fig. 11.7 Cross-section micrographs of (**a**) APK, (**b**) ACGK, and (**c**) ACPK cement after 72 days of implantation

On the contrary, the biodegradation profile of APK was almost identical to the AP, and the organic components did not penetrate deeply into the cement. These phenomena suggested that both mineral absorption and precipitation were induced by the organic components and VK2 in the APK cement. Nonetheless, only absorption was observed on the AP cement. The AP and APK cements were composed almost entirely of inorganic components, and the formulation and geometrical structures of the cement are different to natural bone; as a result bone growth factors might be not affected in the formation of bone.

11.4 Skeletal Bone Cell Scaffold Based on Apatite/Collagen Composite Cements

The geometrical structure of pores in implantable artificial bone affects bone regeneration, since bone-related cells grow and proliferate more effectively in interconnected porous materials, such as coral-modified implants made of calcium phosphate and porous β-TCP ceramics. Interconnective pores in coral-like materials

Fig. 11.8 Photograph of ACP block

are therapeutically effective for bone regeneration in the body through the introduction of bone cells and blood vessels [11, 12]. Notably, interconnective porous biomaterials are useful as a scaffold for bone cell cultures for implant. Kuboki et al. [13] discovered the various types of interconnective voids, and pores in artificial bone enhanced the transition from artificial material to natural bone. These voids played a key role in stimulating tissue invasion and biocompatibility. Based on the test results, it can be suggested that continuous voids supported the formation of new bone by allowing the bone cells and/or tissues to penetrate into the voids more readily and the growth of new blood vessels commences.

11.4.1 Biodegradation of Scaffold Based on Apatite/Collagen Composite Cements with Interconnective Macropores in Rats

Since artificial bones are fabricated with favorable properties using apatite/collagen composite with connective voids, these devices could be utilized as a bone cell scaffold to culture bone marrow extracted from patients for bone regenerative medicine. Artificial bone cement with interconnecting pores as a cell scaffold device was therefore prepared based on the AC cement and its biocompatibility investigated after implantation into rats.

The ACP blocks were prepared as follows [14]: cement bulk powders were mixed homogeneously with 25 mM phosphoric acid to form a paste and poured into a mold ($10 \times 10 \times$ depth mm) containing an organized stainless steel needlelike male dies 600 μm in diameter. The mold is then stored and hardened at 37 °C and 100 % relative humidity for 24 h. The cement blocks with voids were obtained after removing the pins as shown in Fig. 11.8. The APN and ACN blocks were used to harden the AP and AC cement pastes in the mold ($10 \times 10 \times$ depth mm) without pins, respectively.

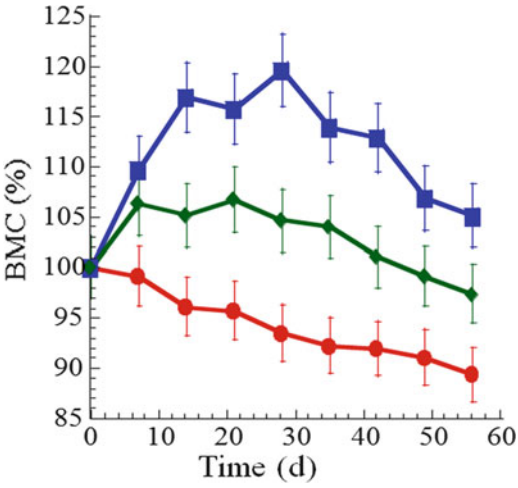

Fig. 11.9 Plot of time versus changes in BMC of cement blocks implanted in rats (■, ACC; ♦, ACN; •, APN)

The XRD result indicated that the calcium phosphates from ACN, ACC, and APN transformed into biological HAp with no peak due to the presence of raw materials, as previously reported [7]. The result of scanning electron microscopy with electron probe microanalyzer revealed the ACC cement has a smooth surface with particles less than 1–2 μm in size and is similar to natural bone [15]. It was also discovered that the geometrical structure of the implants has an effect on the behavior of their biological absorption. The microporosities of the APN and ACN measured using mercury porosimetry were found to be around 40 %, similar to the value previously published [14]. Therefore, the total porosity of the ACC cement was calculated to be approximately 64 % by combining the micro- and macropores which are 40 % and 23 %, respectively.

After the artificial bone blocks (ACN, ACC, and APN) were implanted subcutaneously in female SD rats, their BMC profiles were determined by dual energy X-ray absorptiometry (Fig. 11.9). The analysis revealed the BMC of ACC increased rapidly to around 120 % after 28 days but dropped to 105 % after 56 days. A similar trend was also observed for the ACN cement as their BMC rose to approximately 110 % after weeks 1–3 and at day 56 the BMC was around 98 %. In contrast, the BMC of APN decreased steadily throughout the entire experiment, and at day 56 the BMC was recorded to be approximately 90 % (Fig. 11.9).

The bone mineral density (BMD) of the implanted blocks were also measured and the results showed the density of ACC increased to around 108 % after 42 days and then declined significantly (Fig. 11.10). A gradual decrease was observed for the ACN cement during a 6-week period, and at the end of day 42, the BMD was approximately 92 %. Moreover, the BMD of APN remained unchanged during the first 4 weeks of the experiment but then the BMD steadily decreases and by day 56 it was around 94 %.

Based on these results, it is clear that the cement system will ultimately determine the changes in the BMD profile. During the latter stages of the experiment, a

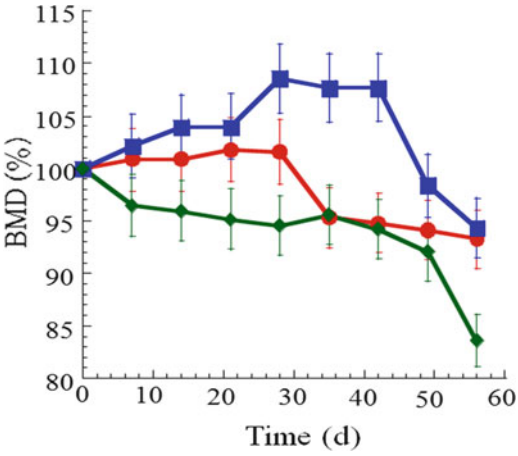

Fig. 11.10 Plot of time versus the changes in BMD of cement blocks implanted in rats. ■, ACC; ♦, ACN; •, APN

decrease in the BMC and BMD was observed with all the implanted blocks, 40–56 days due to the abdomen, and phagocytized on the surface of macropores by osteoclast-like cells bearing the same resemblance as bone remodeling. Photographs of removed implants also indicated that the deformation of the cement blocks can be considered as an indication of biological activity, the order of activity being ACC > ACN > APN. The results of deformation were consistent with the decrease in BMC after 40–56 days.

11.5 Drug Release from Biodegradable Apatite/Collagen Composite Cements with Interconnective Macropores

To improve biocompatibility, three-dimensional perforated porous apatite/collagen composite cement (ACC) with drug delivery capability was developed. It can be hypothesized that this will be a powerful tool in controlling bone regeneration if we can control the release of bone growth factors during cell culture [16].

11.5.1 Controlled In Vitro Drug Release from Skeletal Bone Cell Scaffold by Interconnective Macropores

The ACC device with drug delivery capability was prepared as follows: the AC cement paste containing an apatite cement bulk powder, 20 % type I bovine collagen, and 3 % indomethacin (IMC) bulk powder was poured into the mold ($10.0 \times 10.0 \times 7.5$ mm) to generate interconnective macropores (0, 20, 40, and 60 stainless needles) and stored at 37 °C and 100 % relative humidity for 24 h. The X-ray diffraction and FT-IR results of the cement blocks suggested that

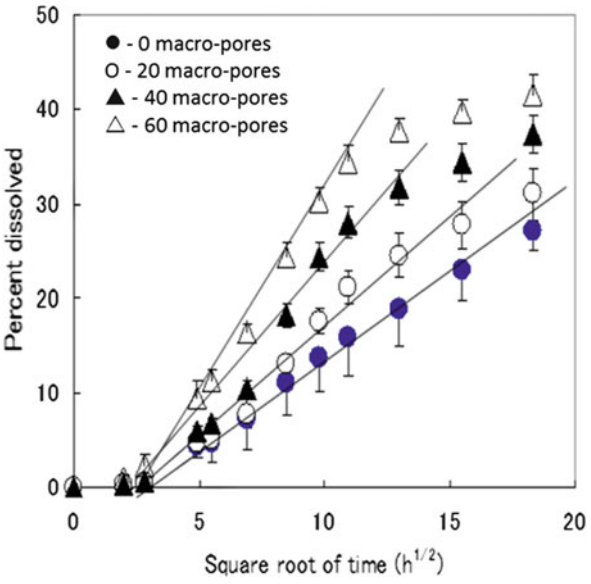

Fig. 11.11 Effects of interconnective macropores on in vitro release of IMC from ACC devices

its characteristics and biocompatibility are comparable to natural bone, and the application of the device as a biodegradation composite for bone repair can be anticipated [14].

To investigate the drug release capability of the ACC devices, tests were carried out in 25 mL of simulated body fluid (SBF) at a pH level of 7.25. The in vitro release of IMC from ACC with 20, 40, and 60 perforated pores in SBF after 336 h was 6.34 ± 0.48, 6.99 ± 0.46, 8.41 ± 0.61, and 9.34 ± 0.51 mg, respectively. By increasing the number of macropores, the release rate of IMC from ACC devices also increased. Since the drug release rate-limiting step of the release from unerosible-homogeneous drug-loaded matrix system was basically the drug diffusion process in the micropores in the matrix, the drug release from the planar surface matrix systems follows the Higuchi equation (Eq. 11.1):

$$M_t = A\sqrt{C_s \frac{D_i \varepsilon}{\tau}(2C_d - \varepsilon C_s)\, t} \tag{11.1}$$

where M_t is the amount of drug released after time t, A is surface are of the device, D is the diffusion coefficient of the drug, C_s is the solubility, C_d is the concentration of drug in the matrix, τ is the tortuosity, and ε is the porosity.

The in vitro IMC release data from ACC with various numbers of macropores were used to plot IMC release against the square root of time (Fig. 11.11). Since the same cement formulation was used for all the ACC devices, the geometrical microstructure (micropore structure) was almost identical for all the devices, and the diffusion parameters of all ACC, such as porosity, drug concentration in the matrices, and pore tortuosity, were almost equal. The only exception is the surface

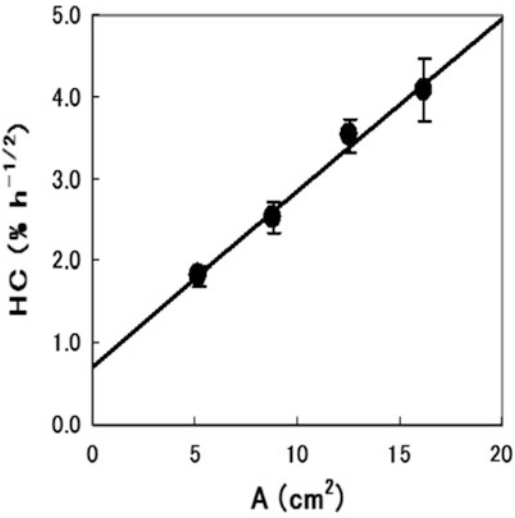

Fig. 11.12 Higuchi-type plot for the in vitro release of IMC from ACC in SBF

area of the devices relative to the geometrical macrostructure of ACC. Therefore, Higuchi equation (Eq. 11.1) can be simplified to form an equation where the surface area of macropores is taken into account as the surface area (A) of the device, and drug release rate of the ACC devices can be manipulated by controlling the value of A (Eq. 11.2):

$$M_t = A \bullet K \bullet \sqrt{t} \tag{11.2}$$

where K is a constant.

The linear relationship between HC and A of ACC as shown in Fig. 11.12 suggested the adequateness of Eq. 11.3, and value of K is derived from the slope of the graph. The results therefore suggest the rate of drug release can be controlled by number of macropores for culturing bone cells:

$$K = \sqrt{C_s \frac{D_i \varepsilon}{\tau} (2C_d - \varepsilon C_s)} \tag{11.3}$$

11.5.2 In Vitro Bone Cell Activity Responsive Drug Release from Biodegradable Apatite/Collagen Bone Cell Scaffold with Interconnective Macropores

As osteoclasts reabsorb bone matrices by exuding acid into the microenvironmental area under the cells [17], it is thus necessary to understand the remodeling of bone grafts by osteoclasts and osteoblasts in order to produce effective implantable apatite cement to deliver drugs to areas affected by osteoporosis.

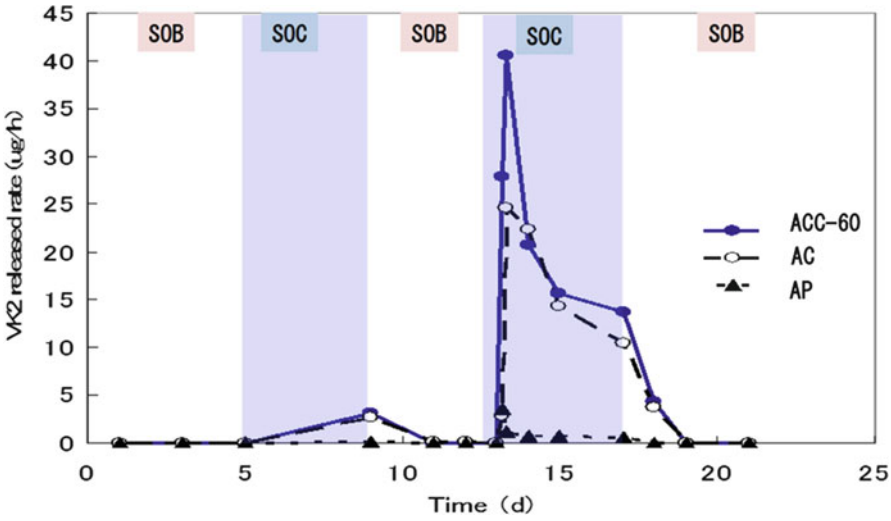

Fig. 11.13 Effects of dissolution mediums on VK2 release from the AP, AC, and ACC cements

Since the crystalline structure of AC was almost the same as natural bone [7], the material was phagocytized at the surface of macropores by bone-like cells, similar to the remodeling of bone.

Therefore, the rapid bioabsorption of AC may be considered to be similar to the biological action of active bone cells [7]. In order to clarify the rule of osteoclasts during drug release from the apatite/collagen nano-composite, we investigated the influence of the dissolution medium on the drug release capabilities of the device based on a physicochemical model for nanoscale bio-interface between bone matrices and bone cells.

The ACP0, ACP20, ACP40, and ACP60 were obtained as follows: the AC cement paste containing an apatite cement bulk powder, 20 % type I bovine collagen, and 2.5 % VK2 bulk powder was cast in the mold ($10.0 \times 10.0 \times 7.5$ mm) to make interconnective macropores (0, 20, 40, and 60 stainless needles) and stored at 37 °C and 100 % relative humidity for 24 h. The X-ray diffraction and FT-IR results suggested that the samples had similar characteristics to natural bone [16].

To clarify the role of bone remodeling in the drug delivery system based on HAp matrices, a physical in vitro dissolution model was established. The drug release profile was investigated in an SBF solution with a pH of 7.25 to simulate osteoblast-like conditions (SOB) and in an acetate buffer with a pH of 4.5 to simulate osteoclast-like conditions (SOC) [16].

Figure 11.13 shows the effect of the dissolution medium on the release of VK2 from AP, AC, and ACC60. It was discovered that virtually no drugs were being released from AC block and ACC-60 in SOB, but the situation was quite the opposite in SOC with significant improvements in the drug release rates. The drug

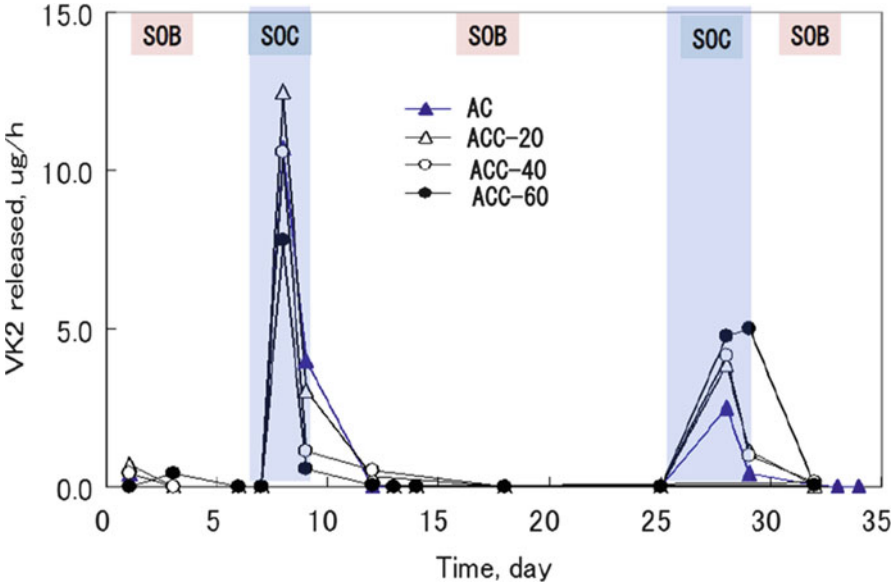

Fig. 11.14 Effects of dissolution medium on the ACC cement with different numbers of macropores

release and calcium phosphate dissolution results suggested that the HAp matrices in the device were dissolved in SOC, and the drug release was accelerated with increasing porosity. In SOB, however, the device was covered with precipitated HAp particles and inhibiting the release of drugs from micropores. The drug release from AC and ACC blocks were dependent on the dissolution medium. However, this is not the case for the AP block.

The drug release from the ACC and AC blocks in SOC was accelerated by the increase in porosity due to the dissolution of HAp matrices, as the biomimetic device had large pores up to 1 μm in size (Fig. 11.13), which could be connected between apatite and collagen matrices. In SOB, on the other hand, the devices were covered with small amounts of fine HAp particles, which inhibited drug release. The drug release results for the AP block revealed that the drug particles did not link together and were encapsulated in the cement matrices.

The relationship between macropore numbers of ACC block and the dissolution medium responses to VK2 release is shown in Fig. 11.14. Based on the drug release profiles, it can be hypothesized that the rate of drug release is dependent on the dissolution medium, and the results were repeated twice in SOC. For ACC, the maximum drug release rate in SOC was more or less proportional to the number of macropores.

Significant deformation of the ACC block was believed to be caused by a repeatable drug release in SOC and SOB (Fig. 11.14). The phenomena might be related to the bone cell activities and the responses to drug release from the cement

device, given that the in vitro drug release experiments can be thought of as a physicochemical model for the remodeling of bone matrices by osteoblast and osteoclast cells. Perforated pores of the devices may possibly be used to control the release of drugs and could be utilized as a bone cell scaffold.

Acknowledgments The author would like to deeply thank Prof. William I. Higuchi, University of Utah for his great leadership to our international collaboration research. The author thanks Professor Hiroyuki Ohshima, Tokyo University of Science, and Dr. Atsuo Ito, NIAIST, for their scientific advice. The author thanks Mr. Ryuhei Hirano, Mr. Hideyuki Hamada, Mr. Hidenori Nakagawa, and Mr. Tomoaki Kuninaga for their experimental works.

References

1. Baron R, Vignery A, Horowitz M (1987) Lymphocytes, macrophages and the regulation of bone remodeling. In: Peck WA (ed) Bone and mineral research. Annual Elsevier, Amsterdam, pp 209–279
2. Aoki H (1994) Medical applications of hydroxyapatite. Ishiyaku EuroAmerica Inc., Tokyo, p 156
3. Miyamoto Y, Ishikawa K, Takechi M, Toh T, Yuasa T, Nagayama M, Suzuki K (1998) Basic properties of calcium phosphate cement containing atelocollagen in its liquid or powder phases. Biomaterials 19:707–715
4. Kikuchi M, Itoh S, Ichinose S, Shinomiya K, Tanaka J (2001) Self-organization mechanism in a bone-like hydroxyapatite/collagen nanocomposite synthesized in vitro and its biological reaction in vivo. Biomaterials 22:1705–1711
5. Itoh S, Kikuchi M, Koyama Y, Takakuda K, Shinomiya K, Tanaka J (2002) Development of an artificial vertebral body using a novel biomaterial, hydroxyapatite/collagen composite. Biomaterials 23:3919–3926
6. John A, Hong L, Ikada Y, Tabata Y (2001) A trial to prepare biodegradable collagen-hydroxyapatite composites for bone repair. J Biomater Sci Polym 12:89–705
7. Otsuka M, Kuninaga T, Otsuka K, Higuchi WI (2006) Effect of nanostructure on biodegradation behaviors of self-setting apatite/collagen composite cements containing vitamin K_2 in rats. J Biomed Mater Res B App Biomater 79B:176–184
8. Chhettry A, Wang Z, Hsu J, Fox JL, Baig AA, Barry AM, Zhuang H, Otsuka M, Higuchi WI (1999) Metastable equilibrium solubility distribution of carbonated apatite as function of solution composition. J Colloid Int Sci 218:57–67
9. Shiraki M, Shiraki Y, Aoki C, Miura M (2000) Vitamin K2 (menatetrenone) effectively prevents fractures and sustains lumbar bone mineral density in osteoporosis. J Bone Miner Res 15(3):515–521
10. Shiomi S, Nishiguchi S, Kubo S, Tamori A, Habu D, Takeda T, Ochi H (2002) Vitamin K2 (menatetrenone) for bone loss in patients with cirrhosis of the liver. Am J Gastroenterol 97(4):978–981
11. Delloye C, Cnockaert N, Cornu O (2003) Current concepts review, bone substitutes, an overview. Acta Orthop Belg 69:1–8
12. Miyai T, Ito A, Tamazawa G, Matsuno T, Sogo Y, Nakamura C, Yamazaki A, Satoh T (2008) Antibiotic-loaded poly-ε-caprolactone and porous β-tricalcium phosphate composite for treating osteomyelitis. Biomaterials 29:350–358
13. Kuboki Y, Jin Q, Kikuchi M, Mamood J, Takita H (2002) Geometry of artificial ECM: sizes of pores controlling phenotype expression in BMP-induced osteogenesis and chondrogenesis. Connect Tissue Res 43:529–534

14. Otsuka M, Nakagawa H, Otsuka K, Ito A, Higuchi WI (2013) Effect of geometrical structure on the in vivo quality change of a three-dimensionally perforated porous bone cell scaffold made of apatite/collagen composite. J Biomed Mater Res B Appl Biomater 101B(2):338–345
15. Otsuka M, Nakagawa H, Ito A, Higuchi WI (2010) Effect of geometrical structure on drug release rate of a three-dimensionally perforated porous apatite/collagen composite cement. J Pharm Sci 99(1):286–292
16. Otsuka M, Hirano R (2011) Bone cell activity responsive drug release from biodegradable apatite/collagen nano-composite cements, – in-vitro dissolution medium responsive vitamin K2 release colloids and surfaces B. Biointerfaces 85(2):338–342
17. Väänänen HK, Zhao H, Mulari M, Halleen JM (2000) The cell biology of osteoclast function. J Cell Sci 113(Pt 3):377–381